Pergamon

PII: S0277–5387(96)00590–6

Polyhedron Vol. 16, No. 14, pp. 2341–2351, 1997

0277–5387/97 $17.00+0.00

Formation, magnetic properties and structures of copper(II) levulinates

J. D. Zubkowski,[a]* D. Washington,[a] N. Njoroge,[a] E. J. Valente,[b]* T. Cannon,[b] C. D. Parks,[b] P. Berdahl[c] and D. L. Perry[c]

[a]Department of Chemistry, Jackson State University, Jackson, MS 39217, U.S.A.

[b]Department of Chemistry, Mississippi College, Clinton, MS 39058, U.S.A.

[c]Lawrence Berkeley National Laboratory, University of California, Berkeley, CA 94720, U.S.A.

(Received 20 September 1996; accepted 2 December 1996)

Abstract—The syntheses and characterizations of a series of copper(II) levulinic acid complexes are reported. The structure of $[Cu_2(O_2C(CH_2)_2COCH_3)_4]_n({}^-O_2C(CH_2)_2COCH_3$ = lev), **1**, and the products of its reaction with pyridine, 2,2′-dipyridine and triphenylphospine have been determined by single crystal X-ray diffraction. The reaction with pyridine leads to $[Cu(H_2O)(O_2CCH_2CH_2COCH_3)_2(NC_5H_5)_2]$, **2**. Reaction with 2,2′-dipyridine leads to $[Cu(O_2CCH_2CH_2COCH_3)_2(N_2C_{10}H_8)]$, **3**. When $Cu_2(lev)_4$ is reacted with PPh_3 the product is $[Cu_2(O_2CCH_2CH_2COCH_3)_4\{(\mu\text{-}O_2CCH_2CH_2COCH_3)(Cu(PPh_3)_2\}_2]$, **4**. Solid-state magnetic susceptibility studies are described for **1** and **4** from 5–300 K, which suggests the system is similar to the known copper(II) acetates. Fitting parameters are $-J/k = 410(10)$ K and $g = 2.10(5)$ for **1** and $-2J/k = 425(20)$ K and $g = 2.25(10)$ for **4**. Compounds **1**, **2**, **3** and **4** have been studied by single crystal X-ray crystallography. © 1997 Elsevier Science Ltd. All rights reserved.

Keywords: crystal structures; copper complexes; levulinic acid; magnetic properties; copper carboxylates; nitrogen donor ligands.

Metal carboxylates are a long studied and structurally diverse class of compounds. This arises in part from the several bonding modes used by carboxylate as a ligand to transition metal ions [1]. Copper(II) carboxylate compounds have been the subject of many studies. Several reviews on copper carboxylate compounds discuss the nature and magnitude of magnetic interactions and its dependence on structural properties [23]. There have been many published reports of strong anti-ferromagnetic interactions in dimeric copper(II) carboxylate complexes. The most thoroughly investigated of these compounds is hydrated copper acetate, for which Figgis and Martin [3] found $g = 2.13$ and $-2J/k = 408$ K (cited as 286 cm^{-1}). This value is supported by subsequent magnetic studies [4] and by similar value (432 K, 298 cm^{-1}) found with neutron scattering [5]. Doedens reviewed magnetic and structural data on a number of copper(II) dimer carboxylate complexes [6]. In all Cu^{II} carboxylate dimers, the copper magnetic environment is identical, with the exchange coupling ranging from 250 to 555 cm^{-1}. No clear correlation with structure has yet emerged. The present results enlarge the data set for the pursuit of such correlations.

Several related systems have been reported. Copper(I) acetate [7] is planar and polymeric and copper(II) acetate is dimeric and a dihydrate [8]. When the alkyl group on the carboxylate is C_2H_5 or larger, anhydrous compounds can be formed where the apical ligand is a carboxylate oxygen atom [6]. Dinuclear copper carboxylate complexes also occur in a variety of biological systems [9].

We have become interested in γ- and δ-oxocarboxylic acids as ligands in the copper systems. The parent oxoacids may exist in solution as an equilibrium between open and cyclic lactol (pseudoacid) forms depending on their structures. The combination of a metal cation with the open chain carboxylate is anticipated to leave the distal carbonyl function uncomplexed. The apparent hydrated dimer $Cu_2(lev)_4(H_2O)_2$ has been reported but little else is

---

* Authors to whom correspondence should be addressed.

known about the chemistry or structure of the substance [10]. As part of an inquiry into this area, we have prepared and characterized copper(II) levulinate and investigated the products of its reactions with several Lewis bases.

EXPERIMENTAL

General

All chemicals were reagent grade and were used as received. Infrared spectra were recorded as KBr pellets on a PE 16PC FT-IR spectrophotometer. UV-Vis spectra were recorded on a PE Lambda 3B spectrophotometer. NMR spectra were recorded on a GN-300 FT-NMR. The magnetic moment of the copper dimer materials was determined with a Quantum Design Model MPMS SQUID magnetometer (LBNL). The moment was measured while warming the sample from 5 K to 280 K in a field of 1 tesla (T), then cooling the sample to 5 K in a field of 3 or 4 T and finally reducing the field to zero at 5 K. The time was about 30 s for each individual moment determination. A correction was made for the diamagnetic plastic sample container. A small offset was applied to the data so that the moment approached zero at low temperature. The size of the effect was approximately equal to the underlying diamagnetism of the ion cores. Other magnetic susceptibility measurements were determined on a MSB-1 Balance using mercury(II)tetrathiocyanatocobalt(II) as the calibrant.

Synthesis of $[Cu_2(O_2CCH_2CH_2COCH_3)_4]$, (**1**)

The synthesis of the title compound followed the method of Gopalakrishnan and Patel [10] with 98% levulinic acid solution (from Aldrich) in water. The compound was crystallized from a concentrated water solution as dichroic blue–green blocks. IR data: (in KBr, cm^{-1}) 2975 w, 2928 w, 1711 vs, 1587 vs, 1434 vs, 1410 s, 1368 s, 1240 m, and 1167 m. UV–vis: (acetone) 370 nm ($E = 60$) and 680 nm ($E = 150$).

Synthesis of $[Cu(H_2O)(O_2CCH_2CH_2COCH_3)_2(NC_5H_5)_2]$, (**2**)

In 20 cm^3 of wet pyridine, 0.30 grams (0.51 mmol) of **1** was dissolved and its blue color deepened as the solution was stirred for 2 h. The solvent was removed and a fine deep blue solid was isolated. The solid was redissolved in a minimum amount of pyridine/toluene (1 : 5) and chilled at −20°C overnight where deep blue crystals formed. The product was isolated by filtration, 0.34 grams, 73%. IR data (in KBr, cm^{-1}) 3500 br, 3040 w, 2915 w, 1716 vs, 1626 vs, 1437 vs, 1367 s, 1164 m, 1070 m and 690 m. UV–vis: (pyridine) 370 nm ($E = 60$) and 645 nm ($E = 100$).

Synthesis of $[Cu(O_2CCH_2CH_2COCH_3)_2(N_2C_{10}H_8)]$, (**3**)

In 20 cm^3 of toluene, 0.30 grams (0.51 mmol) of **1** and 0.53 grams (1.6 mmol) of 2,2′-dipyridine were dissolved and the blue color of the solution deepened as the solution was stirred for 2 h. A blue-green solid precipitated. The solution was filtered, 0.25 grams, 54%. IR data: (in KBr, cm^{-1}) 3070 w, 2975 w, 2928 w, 1710 vs, 1629 vs, 1444 vs, 1364 s, 1164 m, and 702 m. UV–vis: (acetone) 420 nm ($E = 28$) and 660 nm ($E = 43$).

Synthesis of $[Cu_2(O_2CCH_2CH_2COCH_3)_4\{(\mu\text{-}O_2CCH_2CH_2COCH_3)(Cu(P(C_6H_5)_3)_2\}_2]$, (**4**)

In 20 cm^3 of tetrahydrofuran, 0.30 grams (0.51 mmol) of **1** and 0.43 grams (1.64 mmol) of triphenylphosphine was dissolved. The initially blue solution slowly turned green upon stirring overnight. After concentrating to 5 cm^3, 15 cm^3 of hexane was added and the solution was chilled to −20°C overnight. The product was filtered and occurs as deep green crystals, 0.40 grams, 84%. IR data (in KBr, cm^{-1}) 3050 w, 2915 w, 1973 w, 1905 w, 1842 w, 1721 vs, 1637 vs, 1579 m, 1563 m, 1437 vs, 1400 m, 1160 m, 1096 m, 790 m, 696 m and 500 m. UV–vis: (thf) 420 nm ($E = 100$) and 670 nm ($E = 420$). ^{13}C NMR ($CDCl_3$) 30.4 m, 32.0 m, 127.5–134.9 m ($C_6H_5^-$), 211.9 s. ^{31}P NMR ($CDCl_3$) 2.30 broad singlet.

Crystallography

A brief summary of relevant crystallographic details is given in Table 1. Specimens were mounted in capillaries (**2** in contact with aqueous pyridine, **3**) or on slender glass fibers (**1**, **4**). Data was collected on a Siemens R3m/V automated diffractometer with graphite monochromatized Mo-K_α ($\lambda = 0.71073$ Å) [11] radiation to $2\theta = 50°$(**2**–**4**), 70° (**1**). An empirical absorption correction [12] was applied to the data for **3**; minimum and maximum transmission factors 0.92 and 0.32, respectively. Structures were discovered with SHELXS-80 [13] by direct methods or the Patterson function. Final models for each were refined with SHELXL-93 [14] and included positions and anisotropic vibrational factors for all non-H atoms with positions and isotropic vibrational factors for the H-atoms calculated and contributing but not refining. Scattering factors taken from the *International Tables for X-ray Crystallography* [15].

For **1** R_1 (final) was 0.0419, $wR_2 = 0.0936$, goodness-of-fit = 0.572 for 161 variables and the final difference map features spanned +0.61 and −0.46 $e/Å^{-3}$. For **2**, R_1 (final) was 0.0432, $wR_2 = 0.1006$, goodness-of-fit = 0.733 for 577 variables, and the final difference map features spanned +0.43 and −0.66 $e/Å^{-3}$. For **3**, R_1 (final) was 0.0315, $wR_2 = 0.0733$, goodness-of-fit = 1.032 for 142 variables, and the final

Table 1. Structural determination

Compound	1	2	3	4
Emp. Formula	$C_{10}H_{14}CuO_6$	$C_{20}H_{26}CuN_2O_7$	$C_{10}H_{11}Cu_{0.5}NO_3$	$C_{51}H_{51}O_9P_2Cu_2$
Crystal Form	Blue-green plate	Blue violet lathe	Blue rhomboid	Green blocks
Crystal System	Monoclinic	Orthorhombic	Orthorhombic	Triclinic
Space Group	*C*2/c, [no.15]	*Fdd*2, [no. 43]	*Pbcn*, [no. 60]	*P*-1, [no. 2]
a (Å)	29.436 (4)	18.589 (21)	17.122 (9) Å	12.397 (3)
b (Å)	5.1576 (7)	43.240 (50)	8.625 (5)	12.986 (5)
c (Å)	16.398 (4)	5.572 (4)	14.011 (6)	17.734 (7)
α (°)	90	90	90	999.810 (10)
β (°)	91.21 (2)	90	90	103.840 (10)
γ (°)	90	90	90	115.450 (10)
Z	8	8	8	1
V (Å^3)	2489.0 (8)	4479 (8)	2069 (2)	2378 (1)
D_{calc} (Mg/m^3)	1.547	1.394	1.444	1388
Size (mm)	0.4+0.16+0.08	0.65 × 0.2 × 0.04	0.50 × 0.50 × 0.50	0.2 × 0.35 × 0.4
Formula weight (amu)	305.74	469.97	224.97	999.94
Radiation	Mo-K_α (λ = 0.71073 Å)	Mo = K_α (λ = 0.71073 Å)	Mo-K_α (λ = 0.71073 Å)	Mo-K_α (λ = 0.71073 Å)
Scan Type	ω	ω	ω	ω
No. of relections collected	5576	1097	6754	7384
No. of unique reflections	5497	1097	1837	6742
T (°C)	20.0	20.0	20.0	20.0
Solution	Direct methods (ShelXS)	Patterson	Direct methods (ShelXS)	Direct methods (ShelXS)
Refinement Method	Full-matrix least-squares	Full-matrix least-squares	Full matrix least-squares	Full-matrix least-squares
No. of parameters refined	161	139	142	577
Final *R* indices (obs. data)	R_1 = 4.19%	R_1 = 4.50%	R_1 = 3.15%	R_1 = 4.32%
	wR_2 = 9.36%	wR_2 = 9.27%	wR_2 = 7.33%	wR_2 = 10.06%
R indices (all data)	R_1 = 14.56%	R_1 = 6.89%	R_1 = 4.83%	R_1 = 7.92%
	wR_2 = 10.20%	wR_2 = 9.64%	wR_2 = 8.12%	wR_2 = 10.66%
Goodness-of-fit	0.572	0.733	1.037	0.817
a	0.0428	0.0545	0.0386	0.0527
Largest difference peak/hole (e Å^{-3})	0.605, −0.455	0.433, −0.655	0.261, −0.305	0.423, −0.399

$R_1 = \Sigma \| F_o| - |F_c \| / \Sigma |F_o|$, $wR_2 = [\Sigma(wF_o^2 - F_c^2)^2 / \Sigma(wF_o^4)]^{1/2}$.

Goodness-of-Fit = $[\Sigma(w|F_o| - |F_c|)^2/(n_o - n_v)]^{1/2}$ where n_o = number of observations, n_v = number of parameters and w = weights.

weight = $1/\sigma^2(F_o^2) + (a^*P)^2 + 0.000^*P$, where $P = (\max(F_o^2, 0) + 2^*F_c^2)/3$.

difference map features spanned +0.26 and −0.31 e/Å^{-3}. For **4**, R_1 (final) was 0.0450, wR_2 = 0.0927, goodness-of-fit = 0.572 for 139 variables, and the final difference map features spanned +0.43 and −0.66 e/Å^{-3}. Tables 2–5 contain selected bond length and interbond angles in the respective structures. Atomic coordinates have been deposited with the Cambridge Crystallographic Data Centre.

RESULTS AND DISCUSSION

The parent compound, $Cu_2(lev)_4$, was synthesized and then used as the starting material in the synthesis of the three derivative copper levulinates, **2**–**4**.

Structure of $[Cu_2(O_2CCH_2CH_2COCH_3)_4]$, (**1**)

$Cu_2(lev)_4$ can be prepared in excellent yields from the reaction of copper(II) carbonate and levulinic acid in water. Originally this material had been identified as a dihydrate, $Cu_2(lev)_4(H_2O)_2$, based on its IR spectrum [10]. No $\nu_{(OH)}$ was reported, but the $\nu_{(C=O)}$ at 1724 cm^{-1} could be assigned to the uncoordinated carbonyl group, and the strong features at 1587 and 1434 cm^{-1} were assigned to ν_a and $\nu_{s(OCO)}$ vibrations, respectively, with the former coinciding with the $\delta_{(HOH)}$. In our hands, no $\nu_{(OH)}$ is observed, and a feature at 1587 cm^{-1} appears to be the uncontaminated $\nu_{a(OCO)}$ vibration. This suggests that the complex is anhydrous, which was subsequently confirmed by deter-

Table 2. Selected bond lengths (Å) and angles (°) for **1**

Cu—Cu(a)	2.5870(7)	Cu—O(4a)	2.010(2)
Cu—O(1)	1.937(2)	Cu—O(4a)	2.223(2)
Cu—O(2)	1.939(2)	Cu···Cu(c)	3.22
Cu—O(3)	1.960(2)		
O(1)—Cu—O(2)	169.58(9)	O(3)—Cu—O(4b)	109.67(7)
O(1)—Cu—O(3)	88.41(10)	O(4a)—Cu—O(4b)	81.05(8)
O(2)—Cu—O(3)	90.53(10)	O(1)—Cu—Cu(a)	83.05(7)
O(1)—Cu—O(4a)	89.50(9)	O(2)—Cu—Cu(a)	86.55(7)
O(2)—Cu—O(4a)	89.60(9)	O(3)—Cu—Cu(a)	86.98(5)
O(3)—Cu—O(4a)	169.11(7)	O(a)—Cu—Cu(a)	82.16(5)
O(1)—Cu—O(4b)	90.86(8)	O(4b)—Cu—Cu(a)	162.18(5)
O(2)—Cu—O(4b)	99.25(8)		

Table 3. Selected bond lengths (Å) and angles (°) for **2**

Cu—O(2)	1.922(5)	O(1)···H(4ab)	1.94(1)
Cu—N(1)	2.040(6)	Cu···O(4a)	3.32(1)
Cu—O(4)	2.251(7)	Cu···O(1)	3.18(1)
O(2)—Cu—O(2)	176.8(4)	O(2)—Cu—N(1a)	88.9(2)
O(2a)—Cu—N(1)	88.9(2)	N(1)—Cu—N(1a)	171.7(5)
O(2)—Cu—N(1)	90.8(2)	O(2a)—Cu—O(4)	91.6(2)
O(2a)—Cu—N(1a)	90.8(2)	O(2)—Cu—O(4)	91.6(2)
N(1a)—Cu—O(4a)	94.2(2)	N(1)—Cu—O(4)	94.2(2)
O(4)—Cu—O(4a)	180.0(2)	N(1a)—Cu—O(4)	94.2(2)
O(1)···H(4a)—O(4)	138.0(2)		

Table 4. Selected bond lengths (Å) and angles (°) for **3**

Cu—O(1a)	1.978(2)	Cu—N(1a)	2.002(2)
Cu—O(1)	1.978(2)	Cu—O(2a)	2.437(2)
Cu—N(1)	2.002(2)	Cu—O(2)	2.437(2)
O(1a)—Cu—O(1)	93.83(12)	O(1)—Cu—O(2a)	100.06(7)
O(1a)—Cu—N(1)	94.77(9)	N(1)—Cu—O(2a)	96.18(7)
O(1)—Cu—N(1)	163.75(8)	N(1a)—Cu—O(2a)	106.27(7)
O(1a)1—Cu—N(1a)	163.75(8)	O(1a)1—Cu—O(2)	100.06(7)
O(1)—Cu—N(1a)	94.77(9)	O(1)—Cu—O(2)	58.56(7)
N(1)—Cu—N(1a)	80.43(12)	N(1)—Cu—O(2)	106.27(7)
O(1a)1—Cu—O(2a)	58.56(7)	N(1a)—Cu—O(2)	96.18(7)
		O(2a)—Cu—O(2)	150.58(8)

mination of the solid state structure. The Δ value (the difference between $\nu_{a(OCO)}$ and $\nu_{s(OCO)}$ [16] is related to the bonding mode of a carboxylate ligand. For **1**, Δ is 153 cm^{-1}, which is in the range expected for bridging carboxylate ligands.

From the solid state structure, anhydrous copper(II) levulinate, **1**, forms dimers *via* four bridging levulinate carboxylates. The copper to copper distance is 2.4987(7) Å. The coppers have nearly square pyramid coordination geometry with bonds to four bridging carboxylates and a carboxylate oxygen from a neighboring dimer. The Cu—O distance between dimers is 2.232(2) Å compared to the Cu—O (average) distance within the dimers of 1.962 Å. Thus, anhydrous copper levulinate forms extended chains of dimers along the *b*-axis in the solid. The structure of the repeating unit is shown in Fig. 1. Adjacent nonbonded coppers along the chain are separated by

Table 5. Selected bond lengths (Å) and angles (°) for **4**

CuA—O(2)	1.968(3)	CuB—O(7)	2.104(3)
CuA—O(1)	1.969(3)	CuB—O(8)	2.355(4)
CuA—O(4)	1.973(4)	CuB—P(1)	2.2395(14)
CuA—O(3)	1.977(3)	CuB—P(2)	2.2455(13)
CuA—O(7)	2.167(3)	CuA—Cu(aa)	2.641(2)
		CuA···CuB	3.888(3)

CuAa—CuA···CuB	158	O(1)—CuA—CuAa	84.06(10)
O(2)—CuA—O(1)	167.97(13)	O(4)—CuA—CuAa	87.01(11)
O(2)—CuA—O(4)	88.3(2)	O(3)—CuA—CuAa	81.24(11)
O(1)—CuA—O(4)	88.7(2)	O(7)—CuA—CuAa	177.54(10)
O(2)—CuA—O(3)	90.7(2)	O(7)—CuB—P(1)	115.25(9)
O(1)—CuA—O(3)	89.9(2)	O(7)—CuB—P(2)	112.93(9)
O(4)—CuA—O(3)	168.25(14)	P(1)—CuB—P(2)	129.46(5)
O(2)—CuA—O(7)	94.69(13)	O(7)—CuB—O(8)	58.31(12)
O(1)—CuA—O(7)	97.18(12)	P(1)—CuB—O(8)	115.11(10)
O(4)—CuA—O(7)	95.13(14)	P(2)—CuB—O(8)	102.33(10)
O(3)—CuA—O(7)	96.61(13)		
O(2)—CuA—CuAa	84.15(10)		

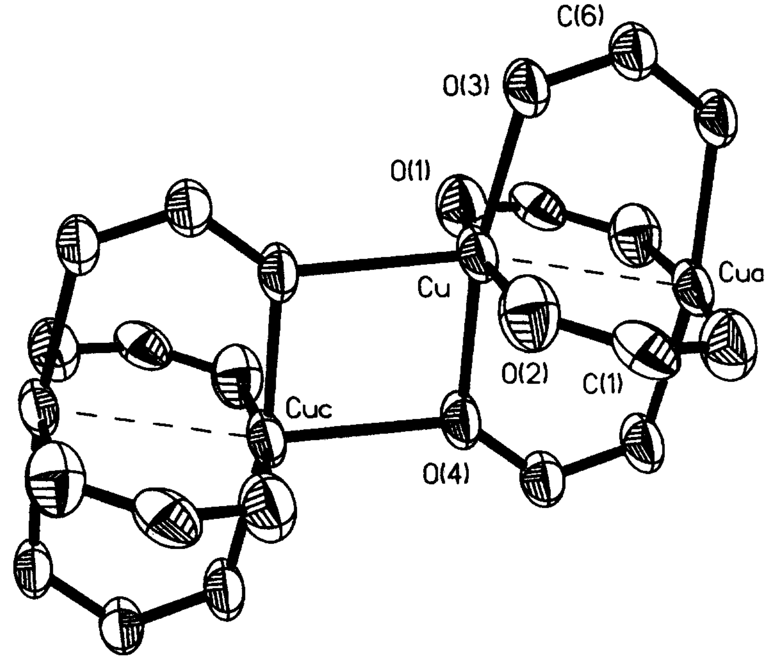

Fig. 1. View of $Cu_2(lev)_4$, **1**, showing coordination sphere. Cu···Cu(a) distance is 2.587(7) Å and Cu···Cu(c) distance is 3.22 Å. Relationship of coppers bridged by the four levulinates is highlighted by a dashed line. Hydrogen atoms and carbon atoms on the levulinate ligands have been removed for clarity (50% ellipsoids).

3.22 Å. Carbonyl groups in the levulinate side-chains are not associated. However, the C—H_α are weakly hydrogen bonded [17] to carboxylate oxygens in a neighboring chain, C(2)—H(2)···O(2′), with the H···O′ distance 2.46 Å and the angle at H 163°. Otherwise, two (of opposing coordination) of the four levulinate side chains are in their fully extended conformations. In the other two, the C_α—C_β bond is in one of the *gauche* conformations. In general, anhydrous copper levulinate has a structure like that of the chain dimeric copper carboxylates with 4, 8, 12 [18,19] chain lengths, and the polymeric copper(II) succinate dihydrate [20].

Structure of $[Cu(H_2O)(O_2CCH_2CH_2COCH_3)_2(NC_5H_5)_2]$, (**2**)

Attempts to prepare dimeric $Cu_2(lev)_4L_2$ species similar to $Cu_2(O_2CCH_3)_4L_2$ with nitrogen donor ligands did not lead to compounds analogous to $Cu_2(O_2CCH_3)_4(NC_5H_5)_2$ [21]. When **1** is dissolved in pyridine the blue solution deepens in color. The product isolated from the reaction is monomeric and there is no evidence for the formation of a dimeric compound under these conditions.

The structure of **2**, Fig. 2(a), has a slightly distorted square pyramid geometry. Copper is coordinated to nitrogen donors of two of pyridine ligands and monodentate oxygen donors of two levulinates and one water. Two nitrogens are coordinated *trans* with a N—Cu—N angle of 171.7(5)°. Bound levulinate oxygens are coordinated to the copper at a distance of 1.922(5) Å, while the uncoordinated oxygens are more distant at 3.184(5) Å. A strong absorption at 1716 cm^{-1} may be assigned to the uncoordinated keto carbonyl group. Strong peaks at 1629 and 1444 cm^{-1} are assigned to the $\nu_{(COO)}$'s. The value of Δ is 185 cm^{-1}. This is in the range expected for unidentate ligands while values of Δ less than 164 cm^{-1}, as in $CH_3CO_2^-$, are expected for metal complexes containing symmetrically bidentate chelating carboxylates. This geometry is also observed in $[CuCl(O_2CPh)_2)(NC_5H_5)_2]$ [22].

The oxygen of the water molecule is axially coordinated to copper at 2.251(7) Å. This distance is comparable to Cu—OH_2 distances in $[Cu(H_2O)$(1,10-phenanthroline)$_2][NO_3]_2$ [23] and in $[Cu(H_2O)$(1,2-bis(9-methyl-1,10-phenantrolin-2-yl)ethane)$][C1O_4]_2$ [24]. Copper has an empty coordination site, but this site is blocked by uncoordinated oxygens of the carboxylates, Fig. 2(b). An apical water of a translationally related molecule (Cu···O 3.12 Å) is hydrogen bonded to both uncoordinated carboxylate oxygens. The hydrogen bonding distances are O(1a)···H(4a′) is 1.944(2) Å, O(1)···O(4a′) is 2.752(2) and the O(1)···H(1a′)—O(4a′) angle is 168.4(2)°.

Structure of $[Cu(O_2CCH_2CH_2COCH_3)_2(N_2C_{10}H_8)]$, (3)

The reaction of **1** with 2,2′-dipyridine (1 : 1 ligand to copper ratio) leads to the breaking of the copper–copper bond and the formation of monomeric $Cu(lev)_2(N_2C_{10}H_8)$. This compound is not isostructural with any of the reported products of the reaction of $Cu_2(O_2CCH_3)_4(H_2O)_2$ and bipyridine, which are reported to be dependent on the ratio of copper to bipyridine [25]. We are currently investigating this relationship for the levulinate system.

Copper in **3** has distorted 4+2 octahedral arrangement of "nitrogen" bonded bipyridyl [26], coordinated oxygens from different levulinate ligands and a coordinated oxygen above and below the plane, Fig. 3. The Cu—N_2O_2 unit is a distorted plane with N(1) and O(1) above the best plane 0.230 Å and 0.28 Å respectively with the symmetry generated atoms an equivalent distance below. Levulinate carboxylates

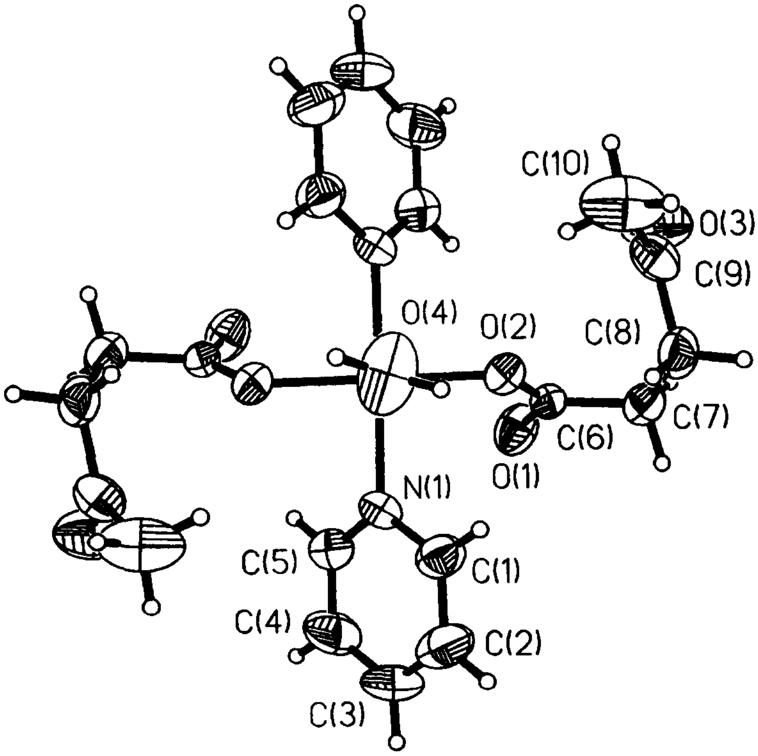

Fig. 2. (a). View of **2** down O(4)—Cu bond axis (50% ellipsoids).

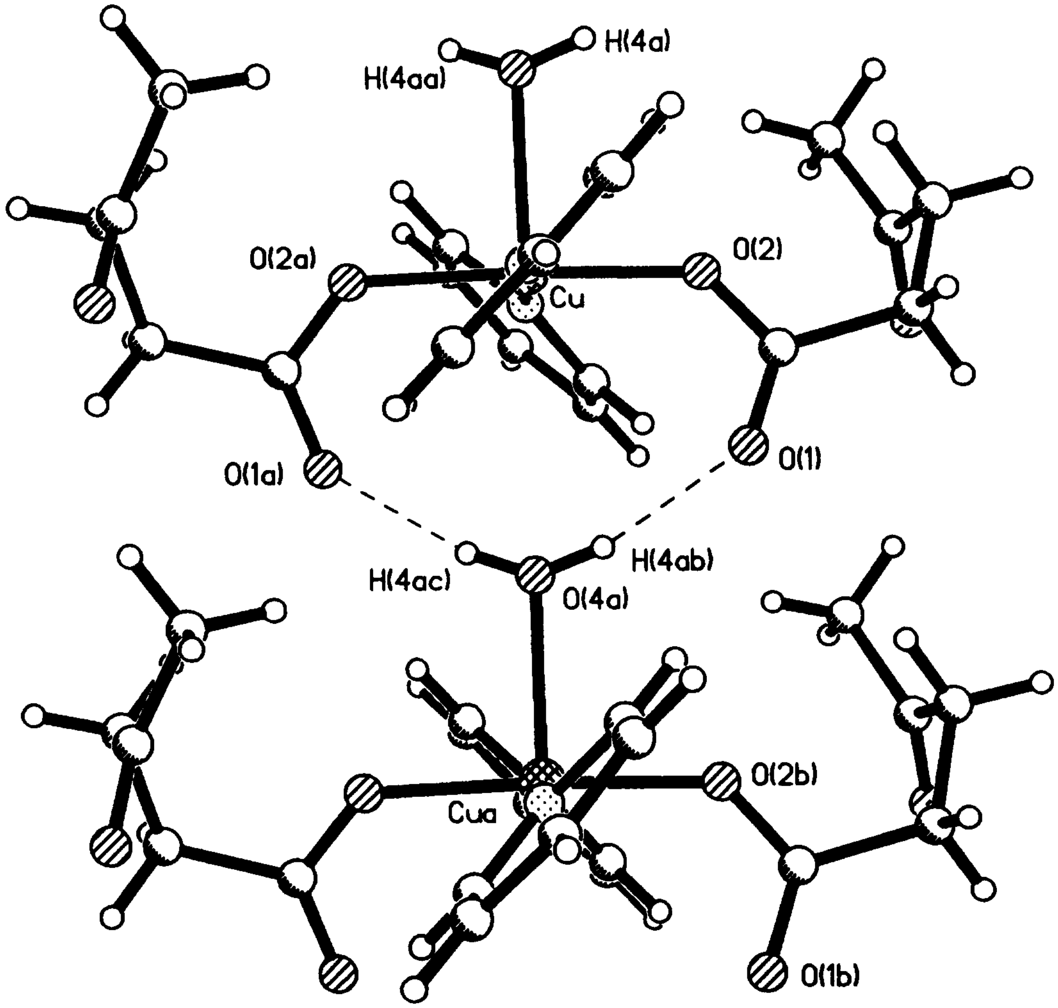

Fig. 2. (b). View of **2** along O(4)—Cu bond axis showing intermolecular interactions: the Cu···O(4′) distance is 3.12 Å and the O(1a)···O(4a′) distance 2.752(2) Å.

bond unsymmetrically, one oxygen of the levulinate is coordinated to the copper at a distance of 1.978(2) Å while the other is more distant at 2.437(2) Å. The long copper to oxygen distance (2.437(2) Å) is in agreement with the expected distance of weakly bonded oxygen [26], the carboxyl stretching frequency difference support this bonding arrangement, ($\Delta = 239\ \mathrm{cm}^{-1}$), which is in the range expected for unidentate ligands. A comparison of carboxylate C—O distances in **1**, **2**, and **3** supports the unsymmetrical bonding. In **1** the C—O distances are 1.264(4) and 1.256(4) Å, which represents a symmetrical bonding arrangement. The unsymmetrically bonded levulinate in **2** has for the coordinated carboxylate oxygen a long C—O distance of 1.267(10) Å and for the uncoordinated carboxylate oxygen a shorter C—O distance of 1.222(9) Å. For **3**, the strongly coordinated carboxylate oxygen has a C—O distance of 1.272(3) Å and the weakly coordinated oxygen has a C—O distance of 1.236(3) Å. A similar structure is observed in [Cu(mhp)$_2$(bipy)], (mhp = 6-methyl-2-pyridonate) [27].

Structure of $Cu_2(O_2CCH_2CH_2COCH_3)_4\{(\mu\text{-}O_2CCH_2CH_2COCH_3)(Cu(PPh_3)_2\}_2$, (4)

When **1** is mixed in solution with triphenylphosphine no change of the blue color is observed until a slight excess of ligand has been added. If stoichiometric amounts of triphenylphosphine and $Cu_2(lev)_4$ are combined, even with gentle heating, unreacted $Cu_2(lev)_4$ is recovered. Once the reaction ensues with the excess ligand, green **4** is produced. This complex is essentially isostructural with the acetate analog, $[Cu_4(O_2CCH_3)_6(PPh_3)_4]$, **5** [28]. On reaction of copper(II)acetate and triphenylphosphine **5** forms by controlling the temperature dependent equilibrium. By controlling the conditions, a Cu^{I} product, $Cu(O_2CCH_3)(PPh_3)_2$ [29], a polymeric compound

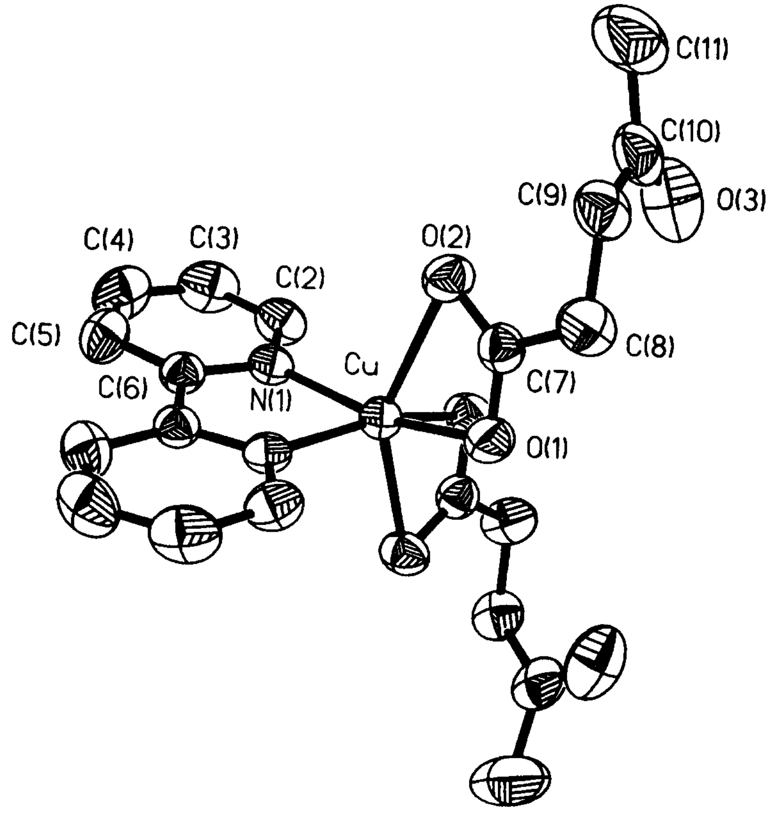

Fig. 3. View of **3** along plane of bipyridyl ligand. Hydrogen atoms have been removed for clarity (50% ellipsoids).

$[Cu(O_2CCH_3)(PPh_3)_2]_n$, or a copper(II) compound, $Cu_2(O_2CCH_3)_4(PPh_3)_2$ [30] forms. The related complex $[Cu_4(O_2CCH_2CH_3)_6(PPh_3)_4(EtOH)_2]$ has also been reported [31].

The coordination sphere of **4** is shown in Fig. 4. The complex has two distinct copper environments. Two copper(II) are bridged by four levulinates ($Cu—O_{average}$ = 1.962 Å) similar to **1**. The Cu(a) oxygen coordination sphere is a distorted square pyramid. The axial coordination site is occupied by a carboxylate oxygen atom from a bridging levulinate, Cu—O 2.167(3) Å. The copper atom is displaced from the basal plane by 0.20 Å towards O(7), the axial levulinate oxygen. Including the adjacent Cu, the

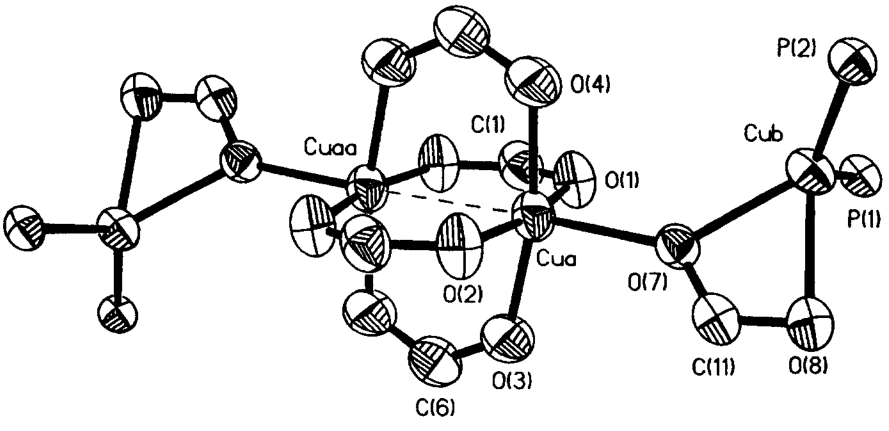

Fig. 4. View of **4**, showing coordination sphere. Relationship of coppers bridged by the four levulinates is highlighted by a dashed line. Hydrogen atoms and carbon atoms on the levulinate ligands have been removed for clarity (50% ellipsoids).

overall Cu(a) coordination is approximately octahedral. The Cu(a)—Cu(aa) distance is 2.641(2) Å and the torsional angle, O(7)—Cu(a)—Cu(aa)—O(7a), is +180°. By comparison, compound **5** has a Cu—Cu distance of 2.642(1) Å, a bridging Cu—O distance of 2.126(4) Å, and a torsional angle of 171.6(10)°.

In **4** the axial levulinate also is bidentate ligand to an $—O_2Cu(PPhh_3)_2$ unit. The Cu(b) atom is in a distorted tetrahedral geometry. The copper atom is coordinated to the axial oxygen, O(7), the alternate carboxylate oxygen of the levulinate axial to Cu(a), O(8), and phosphorous donors of two triphenylphosphine ligands. The O(7)—Cu(b)—O(8) is 58.31(12)°, which is comparable to the O—Cu—O angle in **3**, and in $[(p\text{-tolyl})_3P]_3Cu(O_2NO)$ [32] and $(H_3CCO_2)Cu(PPh_3)_2$ [33].

The infrared spectrum of **4** was assigned by comparison to the reported data for **5**. The absorptions at 1634 and 1434 cm^{-1} ($\Delta = 200\ cm^{-1}$) are assigned to the vibrations of the bridging levulinate ligands in the $Cu_2(lev)_4$ unit. The absorptions at 1576 and 1400 cm^{-1} ($\Delta = 176\ cm^{-1}$) are assigned to the bridging levulinate coordinated between Cu(a) and Cu(b). For $Cu(O_2C\text{-}CH_3)(PPh_3)_2$ the carboxyl stretching frequencies are reported as 1558 and 1415 cm^{-1} ($\Delta = 143\ cm^{-1}$) [30].

Based on ligand charge accounting, the six monoanion ligands seem to require two Cu^{II} and two Cu^{I} atoms in **4**. The geometry of Cu(a) is consistent with an oxidation state of +2, while Cu(b) would appear to be in the +1 oxidation state. This assignment is in agreement with the formal oxidations states calculated from bond valence sum (BVS) calculations [34]. The charge calculated for Cu(a) was +2.08, using the five Cu—O bond lengths. This suggests the formal oxidation state can be assigned as +2. The charge calculated for Cu(b) was +0.93, using the two Cu—O and two Cu—P bond lengths [35]. This is close to expected formal oxidation state of +1. These results are in agreement with formal oxidation states calculated for the mixed-valence copper(I/II) phosphate, Cu_2PO_4 [37]. Similar calculations for **5** and $[Cu_4(O_2CCH_2Ch_3)_6(PPh_3)_4(EtOH)_2]$ yielded oxidation states for the copper(II) atom of +2.08 and +2.15 and for the copper(I) atom of +0.92 and +1.03 respectively.

The solution ^{13}C and ^{31}P NMR of **4** are similar to the spectra reported for $(H_3CCO_2)Cu(PPh_3)_2$ [33]. The ^{13}C NMR has two multiplets at 30.4 ppm and 32.0 ppm assigned as the alkyl carbons, a broad multiplet from 127.5 to 134.0 ppm for the phenyl carbons and a singlet 211.9 ppm assigned to the ketone carbon. The ^{31}P NMR has one broad singlet at 2.30 ppm.

Magnetic properties

The magnetic data were fitted using the following equation, which is based on the standard formalism for dimers with two spin 1/2 (copper(II) ions [37].

$$M/\mu_B = \frac{g\sinh(g\mu_B B/kT)}{(1+2\cosh(g\mu_B B/kT)+(\exp(-2J/kT))}.$$

Here the magnetic moment M, per Cu ion, is expressed in terms of the Bohr magneton (μ_B) spectroscopic splitting factor g, magnetic field B, Boltzmann's constant k, temperature T, and the exchange interaction parameter $2J$ (energy difference between singlet and triplet states of the dimer, negative for antiferromagnetic interaction). For **1** the fit to the 1 T data is excellent, as shown in Fig. 5, using the parameters $g = 2.10 \pm 0.05$ and $2J/k = -410 \pm 10$ K (-285 ± 8 cm^{-1}). The uncertainty in the parameters has been estimated by comparison with a similar but less precise fit to the 3 T data (which gave $g = 2.05$ and $2J/k = -400$ K). The g and $2J$ values translate to an "effective" moment $\mu_{eff} = 1.38\ \mu_B$ at 300 K (the effective moment in Curie's law needed to reproduce the measured 300 K value). The copper coordination sphere is not precisely the same as copper acetate hydrate, even though the match in J-values is quite close. For example, the copper–copper distance is 2.616 Å in copper acetate hydrate, compared with 2.587 Å in **1**.

For **4**, it was expected based on the structure, that half of the copper ions would be in the diamagnetic spin zero Cu^{I} state, whereas the remainder of the copper ions would be present in the form of dimers. This interpretation is borne out by the magnetic moment measurements at 4 tesla, Fig. 6, and shows about twice the magnetic moment seen in Fig. 5. While the moment is increased by a factor of four due to the increased field, and reduced by a factor of 2 because half of the copper ions are non-magnetic. A low temperature T^{-1} peak, presumably due to a small amount of paramagnetic impurities on the sample container,

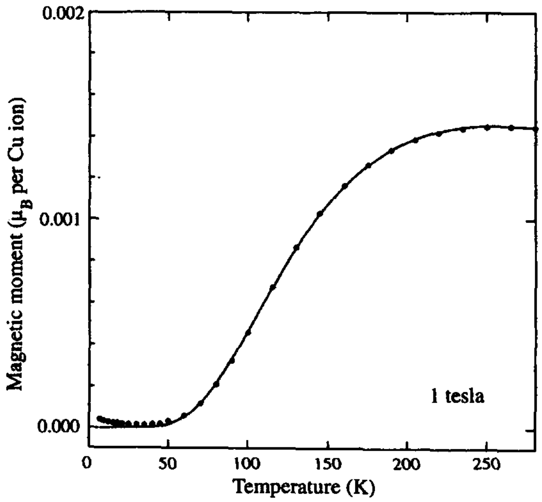

Fig. 5. Magnetic moment per Cu ion versus temperature at 1 tesla for **1**. The continuous curve is the theoretical fit, with parameters given in the text. The slight upturn below 50 K is believed to be an artifact due to parmagnetic impurities on the sample container.

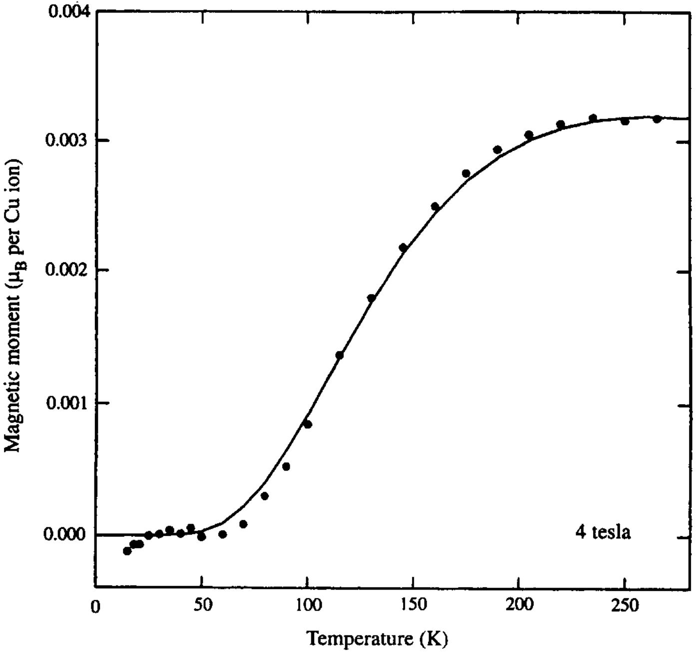

Fig. 6. Magnetic moment per Cu ion versus temperature at 4 tesla for **4**. The continuous curve is the theoretical fit, with parameters given in the text.

was subtracted from the data. The curve fit shown yields $g = 2.24 \pm 0.10$ and $J/k = -4.25 \pm 20$ K (-295 cm^{-1}). Additional data taken at 1 tesla are similar. The values are in agreement with the reported data for **5** of $g = 2.21$ and $2J = -270$ cm^{-1} [25]. The results for **4** lie within the experimental error of the values of the data from **1**, and indicate that the chemical environment of the copper dimers is similar in both cases.

Magnetic susceptibility was determined for all compounds at room temperature on a MSB-1 balance employing the Evans method [38]. From the observed susceptibilities, the magnetic moments were evaluated. The μ_{eff} (B.M., 303 K) for **1** and **4** are 1.39 and 1.54 respectively. For **5** a μ_{eff} (B.M., 292 K) of 1.50 is reported [28]. These values are in the expected range for dimeric copper(II) carboxylates [36]. The monomeric species, **2** and **3**, have μ_{eff} (B.M., 303 K) values of 1.96 and 2.07 respectively which are normal for Cu$^{\text{II}}$ species.

Acknowledgements—We acknowledge support by MBRS-NIH Grant No. GM08047 and the Office of Naval Research (J.D.Z.). Two of the authors (D.L.P. and P.B.) wish to acknowledge support from the U.S. Department of Energy under Contract No. DE-AC0376SF00098. Additional support from the Center for Science and Engineering Education at Lawrence Berkeley National Laboratory through the Director, Office of Energy Research, Division of University and Science Education Programs, from the U.S. Department of Energy, is gratefully acknowledged. We would like to thank Mr A. Jabalameli for obtaining the NMR spectra.

REFERENCES

1. Cotton, F. A. and Wilkinson, G., *Advanced Inorganic Chemistry, 5th Edition.* John Wiley and Sons, New York (1988).
2. (a) Kato, M., Jonassen, H. B. and Fanning, J. C., *Chem. Rev.* 1964, **64,** 99; (b) Hodgson, D. J., *Prog. Inorg. Chem.* 1975, **10,** 173; (c) Melnik, M., *Coord. Chem. Rev.* 1982, **42,** 259; (d) Kato, M. and Mutto, Y., *Coord. Chem. Rev.* 1988, **92,** 45.
3. Figgis, B. N. and Martin, R. L., *J. Chem. Soc.* 1956, 3937.
4. Gregson, A. K., Martin, R. L. and Mitra, S., *Proc. Roy Soc. London A*, 1971, **320,** 473.
5. (a) Gudel, H. U., Stebler, A. and Furrer, A., *Inorg. Chem.* 1979, **18,** 1021; (b) Gudel, R. U., Stebler, A. and Furrer, A., *J. Phys. C* 1980, **13,** 3817.
6. Doedens, R. J., *Progress in Inorganic Chemistry* 21 (Edited by S. J. Lippard). John Wiley, New York (1976).
7. Drew, M. G. B., Edwards, D. A. and Richards, R., *J. Chem. Soc., Chem. Commun.* 1973, 124.
8. De Meester, P., Fletcher, S. R. and Skapski, A. C., *J. Chem. Soc., Dalton Trans.* 1973, 2575.
9. (a) Solomon, E. I., in *Copper Proteins* (Edited by T. G. Spiro) p. 41. Wiley, New York (1981); (b) Kitajima, N., Fijisawa, K. and Morooka, Y., *J. Amer. Chem. Soc.* 1989, **111,** 8975; (c) Tyklar, Z. and Karlin, K. D., *Acc. Chem. Res.* 1989, **22,** 241.
10. Gopalakrishnan, J. and Patel, C. C., *Inorg. Chem.* 1967, **11,** 2111.
11. Diffractometer data collection controlled by P3-PC version (Siemens Analytical X-Ray Instruments, Inc.) Madison, WI.

12. SHELXA-90 ver. 1 (Siemens Analytical X-Ray Instruments, Inc), Madison, WI.
13. Sheldrick, G. M., *Acta Crystallogr.* 1990, **A46,** 467.
14. Sheldrick, G. M., *SHELXL-93: Program for Crystal Structure Refinement.* Göttingen University, Göttingen, Germany (1993).
15. *International Tables for X-ray Crystallography.* Birmingham, Kynoch Press (Klewer Academic Publishers, Dordrecht, The Netherlands) (1987).
16. Nakamota, K., *Infrared and Raman Spectra of Inorganic and Coordination Compounds, 4th Edition.* Wiley-Interscience, New York (1986).
17. Vinogradav, S. N. and Linnell, R. H., *Hydrogen Bonding.* Van Nostrand Reinhold, New York (1971).
18. (a) Lomer, T. R. and Perera, K., *Acta Cryst.* 1974, **B30,** 2912; (b) Lomer, T. R. and Perera, K., *Acta Cryst.* 1974, **B30,** 2913.
19. Bird, M. J. and Lomer, T. R., *Acta Cryst.* 1972, **B28,** 242.
20. O'Conner, B. H. and Maslen, E. N., *Acta Cryst.* 1966, **20,** 824.
21. (a) Hanic, F., Stempelova, D. and Hanicova, K., *Acta Cryst.* 1964, **17,** 633; (b) Barclay, G. A. and Kennard, C. H. L., *J. Chem. Soc.* 1961, 5244; (c) Petric, M., Leban, I. and Segedin, P., *Polyhedron* 1993, **12,** 1973.
22. Speir, G., Fulop, V., *J. Chem. Soc., Chem. Commun.* 1990, 905.
23. Catalan, K. J., Jackson, S., Zubkowski, J. D., Perry, D. L., Valente, E. J., Feliu, L. A. and Polanco, A., *Polyhedron* 1995, **14,** 2165.
24. Yao, Y., Perkovic, M. W., Rillema, D. P. and Woods, C., *Inorg. Chem.* 1992, **31,** 3956.
25. (a) Hathaway, B. J., Ray, N., Kennedy, D., O'Brien, N. and Murphy, B., *Acta Cryst.* 1980, **B36,** 1371; (b) Christou, G., Perlepes, S. P., Libby, E., Folting, K., Huffman, J. C., Webb, R. J. and Hendrickson, D. N., *Inorg. Chem.* 1990, **29,** 3657; (c) Perlepes, S. P., Huffman, J. C. and Christou, G., *Polyhedron* 1992, **11,** 1471; (d) Perlepes, S. P., Libby, E. Streib, W. E., Folting, F. and Christou, G., *Polyhedron* 1992, **11,** 923.
26. Wells, A. F., *Structural Inorganic Chemistry 5th Edn.* Oxford Science Publications Oxford, (1984)
27. Blake, A. J., Gould, R. O., Rawson, J. M. and Winpenny, R. E. P., *J. Chem. Soc., Dalton Trans.* 1994, 2005.
28. (a) Valigura, D., Koman, M., Durcanska, E., Ondrejovic, G. and Mrozinski, J., *J. Chem. Soc., Dalton Trans.* 1986, 2339; (b) Koman, M., Valigura, D., Durcanska, E. and Ondrejovic, G., *J. Chem. Soc., Chem, Commun.* 1984, 381.
29. Darensbourg, D. J., Holtcamp, M. W., Longridge, E. M., Klausmeyer, K. K. and Reibenspies, J. J., *Inorg. Chim. Acta* 1994, **227,** 223.
30. Koman, M., Valigura, D. and Ondrejovic, G., *Acta Cryst.* 1988, **C44,** 601.
31. Dunaj-Juroc, M., Koman, K., Valigura, D. and Ondrejovic, G., *Acta Cryst.* 1995, **C51,** 1082.
32. Pettinari, C., Lobbia, G. G., Sclavi, G., Leonesi, D., Colapietro, M. and Portalone, G., *Polyhedron* 1995, **14,** 709.
33. Hammond, B., Jardine, F. H. and Vohra, A. G., *J. Inorg. Nucl. Chem.* 1971, **33,** 1017.
34. Brown, I. D. and Altermatt, D., *Acta Cryst.* 1985, **B41,** 244.
35. To do this, the r_0 value for Cu^I was calculated as 1.55 for r_{CuO} and 1.79 for r_{CuP} using Brown and Altermatt's algorithm. These r_0 values are considered less accurate than a value determined experimentally.
36. Etheredge, K. M. S. and Hwu, S. J., *Inorg. Chem.* 1995, **34,** 5013.
37. Carlin, R. L., *Magnetochemistry.* Springer-Verlag, Berlin (1986).
38. Evans, D. F., *J. Physics E.: Sci. Instr.* 1974, **7,** 247.